

COMPARISON OF THE EXTENDED KALMAN FILTER AND THE UNSCENTED KALMAN FILTER FOR PARAMETER ESTIMATION IN COMBUSTION ENGINES

Christoph Kallenberger and Haris Hamedović

Corporate Research and Development
Advance Engineering Systems
Robert Bosch GmbH
D-71701 Schwieberdingen, Germany

Abdelhak M. Zoubir

Institute of Telecommunications
Signal Processing Group
Darmstadt University of Technology
D-64283 Darmstadt, Germany

ABSTRACT

In this article, two Kalman filtering techniques, the Unscented Kalman Filter (UKF) and the Extended Kalman Filter (EKF) are applied for cylinder-wise torque estimation. In engine signal processing the problem of engine speed evaluation is one of the main problems of current research for engine control. In this work, two engine speed signals, recorded at the free end and at the flywheel, together with a multi-body model of the crankshaft are used to account for torsional deflections of the crankshaft. In order to estimate cylinder-wise torque, additionally one cylinder pressure signal is used to obtain a parametric torque model. The resulting parameter and state estimation problem allows the comparison of UKF and EKF. The performance of both algorithms was evaluated using measurements from a four cylinder combustion engine. Whilst practical issues still exist, this off-line study showed the feasibility of the approach.

1. INTRODUCTION

The requirements for today's combustion engines are ever increasing. Lower emissions and fuel consumption, as well as increased driving comfort are demanded and require intelligent solutions. Advanced control and diagnostic concepts are being developed in order to reduce fuel consumption and exhaust emissions. These methods need feedback information from each cylinder. In test beds cylinder pressure sensors in all cylinders are usually used. Furthermore, there are also other methods to reconstruct feedback information from the combustion chamber.

In the literature there are three main indirect signal sources considered for pressure or gas torque estimation: engine speed, structure-borne sound and torque. The fluctuations of engine speed deliver information of cylinder-wise torque [1], [2]. Alternatively, structure-borne sound, currently used for knock detection in spark ignition engines, was applied by Villarino [3] for the purpose of pressure reconstruction. Larsson [4] examined pressure reconstruction considering a torque sensor mounted at the crankshaft.

To further improve the accuracy of these approaches, Hamedović et al. [5],[6] introduced a pressure sensor in one cylinder in addition to the engine speed sensor at the flywheel. They approximated the relationship between pressure and engine speed by a stiff crankshaft model and neglected torsional deflections of the crankshaft. This method is successful in certain operating regions with low torsional oscillations.

At higher engine speeds, the influence of torsional fluctuations increases and disturbs the engine speed signal. This work focuses on developing a new cylinder-wise torque es-

timating method fusing two engine speed signals with a torsional multi-body model of the crankshaft and one pressure signal. Therefore, an inversion of the linear time invariant MIMO system is necessary.

The paper is organized as follows: In section 2 the multi-body model of the crankshaft and its linearization to a linear time invariant MIMO system is explained. In section 3 the system inversion of this MIMO system for cylinder-wise torque estimation is described. A parametric torque model is obtained from the cylinder pressure measurement which allows input torque modelling of the other cylinders. The resulting state and parameter estimation problem is used to compare the Extended Kalman Filter (EKF) and the Unscented Kalman Filter (UKF). The experimental results from using a four-cylinder engine test bed are presented in section 4. Section 5 covers conclusions and future goals of this work.

2. CRANKSHAFT MODELLING

The relationship between gas torque and engine speed is described by the dynamics of the crankshaft. Stiff crankshaft modelling neglects the fact that torsional vibrations influence engine speed, especially at higher engine speeds. This work aims to show improved torque estimation using a multi-body model of the crankshaft according to [7]. The torque balance equation is as follows:

$$\Theta \ddot{\varphi} + \mathbf{D} \dot{\varphi} + \mathbf{K} \varphi = \tau_{ind}(\varphi) + \tau_{mass}(\varphi) + \tau_{load}(\varphi) + \tau_{fric}(\varphi). \quad (1)$$

The matrices Θ , \mathbf{D} , \mathbf{K} are symmetric and represent the rotating moment of inertia, damping and stiffness behavior of the crankshaft. The crank angle vector φ and its derivatives $\dot{\varphi}$, $\ddot{\varphi}$ are found from the torsional movement resulting from the sum of indicated torque τ_{ind} , mass torque τ_{mass} , load torque τ_{load} and friction torque τ_{fric} . Indicated torque $\tau_{ind,l}$ of cylinder l at crank angle φ is caused by the in-cylinder pressure p_l

$$\tau_{ind,l}(\varphi) = (p_l(\varphi) - p_0) h\left(\varphi - (l-1) \frac{4\pi}{z}\right) \quad (2)$$

with $h(\varphi) = A r \left(\sin \varphi + \frac{\lambda \sin \varphi \cos \varphi - \mu \cos \varphi}{\sqrt{1 - \lambda^2 \sin^2 \varphi + 2 \lambda \mu \sin \varphi - \mu^2}} \right)$, where p_0 is the ambient pressure, z the number of cylinders, l the cylinder index according to the firing order, A the piston area, r the crank radius, λ the connecting rod ratio, and μ the axial offset ratio [6]. In the following, $z = 4$ is used, since the test bed is a four-cylinder engine. Furthermore cylinder numbering is done according to the geometrical order of the cylinders (starting with 1 at the free end side of the crankshaft) if not mentioned otherwise.

The mass torque results from the oscillating parts of the crankshaft, such as pistons and rods and increases with engine speed. The mass torque of cylinder l is calculated as follows:

$$\begin{aligned} \tau_{mass,l}(\varphi) &= -\theta_l(\varphi) \frac{d\dot{\varphi}}{d\varphi} \dot{\varphi} - \frac{1}{2} \frac{d\theta_l(\varphi)}{d\varphi} \dot{\varphi}^2 \\ &\approx -\frac{m_l}{2} r^2 \frac{d\dot{\varphi}}{d\varphi} \dot{\varphi} - \frac{1}{2} \frac{d\theta_l(\varphi)}{d\varphi} \dot{\varphi}^2 \end{aligned} \quad (3)$$

where $\theta_l(\varphi)$ stands for the moment of inertia of the oscillating parts of a cylinder l and m_l for the corresponding mass. The moment of inertia $\theta_l(\varphi)$ can be approximated by $\frac{m_l}{2} r^2$ according to Schagerberg [8].

Figure 1 shows the multi-body dynamic crankshaft model. Neighboring rotating moments of inertia θ_i , θ_j of the dampers, the free end, the four cylinders and the flywheel are connected by relative stiffness and damping coefficients $k_{i,j}$ and $d_{i,j}$. The corresponding stiffness and damping torques are proportional to the crank angle or, rather, the crank angle velocity. The absolute damping coefficients d_i introduced by [7] reflect the piston friction in the cylinders. In this work the absolute damping coefficients are included into the total friction torque. For steady state, load and friction torque are assumed to be constant and can be estimated from the mean value of the total indicated torque.

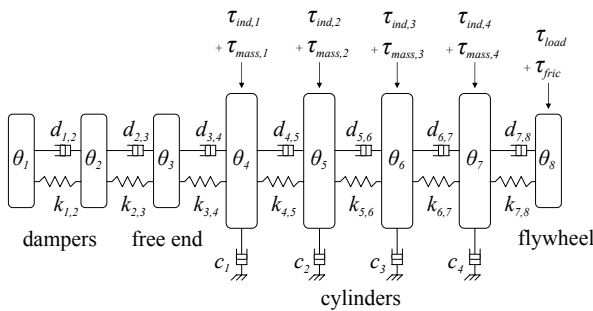


Fig. 1. Crankshaft model for $z = 4$ cylinders

The multi-body dynamic crankshaft model can then be described by the following nonlinear differential state space equations:

$$\begin{aligned} \dot{\underline{x}} &= \mathbf{A}(\underline{x}) \underline{x} + \underline{b}(\underline{x}, \underline{u}) \\ \underline{y} &= \mathbf{H} \underline{x} \end{aligned} \quad (4)$$

with state vector $\underline{x} = [x_1^T \ x_2^T]^T = [\varphi^T \ \dot{\varphi}^T]^T$. The nonlinear effects are caused by the mass torque. The input vector \underline{u} and the output vector \underline{y} are chosen as follows:

$$\begin{aligned} \underline{u} &= [\tau_{ind,1}, \dots, \tau_{ind,4}, \tau_{load}]^T \\ \underline{y} &= [\dot{\varphi}_{fe}, \dot{\varphi}_{flwh}]^T. \end{aligned} \quad (5)$$

Available measurement signals are the angle velocities at the free end $\dot{\varphi}_{fe}$ and at the flywheel $\dot{\varphi}_{flwh}$. For the free end, an optical sensor is used. Engine speed at the flywheel is measured using a toothed gear with 60 teeth.

Assuming identical mass torque at each cylinder allows the formulation of the mass torque as an additional input to the system and a linearized approximation can be found:

$$\dot{\underline{x}} = \mathbf{A} \underline{x} + \underline{b}(\underline{x}, \underline{u}) \quad (6)$$

with $\underline{u}^* = [\tau_{ind,1} + \tau_{mass,1}, \dots, \tau_{ind,4} + \tau_{mass,4}, \tau_{load}]$.

The mass torques $\tau_{mass,1}$ to $\tau_{mass,4}$ are 180 crank angle degrees (CAD) phase shifted according to the geometrical order of the cylinders. The matrix \mathbf{A} depends on the spring, damping and rotating inertia coefficients. The mass torque can be calculated from the engine speed measurement by (3).

The linearized crankshaft model is part of the torque estimation approach described in the next section.

3. SYSTEM INVERSION USING A PARAMETRIC TORQUE MODEL

In order to estimate cylinder-wise torque it is necessary to invert the system equations (6). Having free end and flywheel engine speed signals, as well as one pressure signal available transforms this problem into an inversion of a linear time invariant MIMO system with five inputs (indicated torque of cylinders 1-4 and load torque) and two outputs (engine speed signals).

The system inversion approach in this work uses a parametric torque model which is obtained from the pressure measurement in one cylinder. Therefore one input of the MIMO system is known. Torque estimation is possible via parameter estimation of the cylinder-wise torque model.

Section 3.1 describes the parametric torque model and its transformation to a design model for a state and parameter estimator. In section 3.2 implementation issues of the EKF and the UKF are explained.

3.1 Parametric Torque model

In order to build the parametric torque model the cylinder pressure needs to be processed. Without loss of generality the measured cylinder pressure in this work is chosen to be cylinder one according to the geometrical order at the crankshaft. A pressure decomposition according to [6] is conducted.

This decomposition is based on the fact that measured pressure traces at one operating point are identical for each operating cycle in the region before the combustion. This region is dominated by the compression in the cylinder. The compression pressure $g(\varphi)$ can be described by the following adiabatic pressure model:

$$g(\varphi) V(\varphi)^\kappa = C, \quad (7)$$

where κ is the adiabatic exponent, $V(\varphi)$ is the stroke volume and C is a constant. The parameters κ and C can be estimated using a least square estimation method assuming that cylinder and compression pressure traces are equal in the crank angle region of -180 to 0 before injection. [6]. The difference between the measured pressure $p(\varphi)$ and the compression pressure $g(\varphi)$ is called the combustion pressure $f(\varphi)$. In the following, this notation is used for the pressure decomposition of cylinder 1.

Figure 2 illustrates the decomposition of the measured pressure into compression and combustion pressure. The compression component depends mainly on the manifold pressure and the operating conditions. Since those are widely

constant during one engine cycle the compression component can be assumed to be identical for all cylinders in this region.

Next, the corresponding combustion and compression torque components $\tau_f(\varphi)$ and $\tau_g(\varphi)$ can be calculated by:

$$\begin{aligned}\tau_f(\varphi) &= f(\varphi)h(\varphi) \\ \tau_g(\varphi) &= (g(\varphi) - p_0)h(\varphi),\end{aligned}\quad (8)$$

where p_0 is the ambient pressure and $h(\varphi)$ the geometrical factor according to (1).

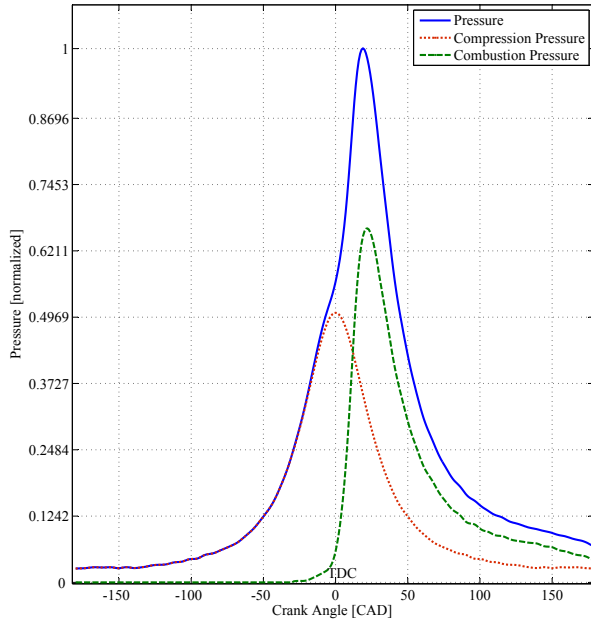


Fig. 2. Pressure decomposition into a compression and a combustion component (TDC: top dead center). All components are normalized to the peak pressure.

Figure 3 illustrates the separation of the indicated torque into combustion and compression torque. From considerations above the compression torque $\tau_g(\varphi)$ of cylinder 1 is used to approximate the compression torques of the other 3 cylinders. The compression torques τ_{comp} are then formulated as known inputs to the crankshaft system (6):

$$\tau_{comp} = \tau_g(\varphi - (l-1)\pi) \approx \tau_{comp,l} \Big|_{l=2,3,4} \quad (9)$$

Considerations of the combustion components in figure 3 allows a cylinder-wise segmentation of one operating cycle. This is important for the design of the parameter estimators further explained in sections 3.2.

In order to estimate the combustion components of cylinder l (2-4) in firing order, the combustion torque of cylinder 1 is used to build the following combustion torque model:

$$\tau_{comb,l}(\underline{\vartheta}_l, \varphi) = \alpha_l \tau_f(\varphi - (l-1)\pi - \delta_l) \quad (10)$$

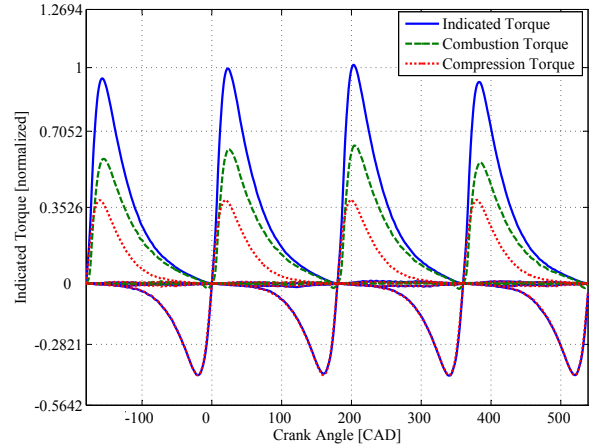


Fig. 3. Separation of indicated torque into combustion and compression torque. All components are normalized to the indicated torque peak of cylinder 1.

The phase constant π is added to shift the combustion torque of cylinder 1 into the corresponding combustion segment of cylinder l . The parameters of the combustion torque model are a scaling parameter α_l and a shifting parameter δ_l which can be combined to a parameter vector $\underline{\vartheta}_l$. These parameters allow the adaptation of the combustion torque according to phase and energy of the combustion.

The unknown load torque of the crankshaft system is assumed to be constant over one engine cycle. It can therefore be estimated through scaling the mean value of the indicated torque of cylinder one:

$$\tau_{load} = \gamma 4 \times \overline{\tau_{ind,1}} \quad (11)$$

The mean value of the indicated torque of cylinder 1 needs to be scaled by the number of cylinders (here 4) to get a good initial load torque estimate. The scaling parameter γ then scales the initial load torque estimate to get a better estimation of the real load torque. Thus a load torque scaling parameter γ is introduced and can be estimated together with the parameter vector $\underline{\vartheta}$ according to the engine speed fluctuations at the free end and at the flywheel.

In order to estimate the cylinder-wise combustion torque of each cylinder, the combustion and load torque models need to be integrated into the system equations of the crankshaft (1). They are discretized and their inputs are split into known and unknown inputs \underline{u}_1 and \underline{u}_2 :

$$\underline{x}_{k+1} = \Phi \underline{x}_k + B_1 \underline{u}_1 + B_2 \underline{u}_2 \quad (12)$$

with the input vectors \underline{u}_1 (known) and \underline{u}_2 (unknown), as well as the discretized system matrix Φ :

$$\begin{aligned}\underline{u}_1 &= [\tau_{ind,1} + \tau_{mass,1}, \tau_{comp} + \tau_{mass,2}, \dots, \tau_{comp} + \tau_{mass,4}] \\ \underline{u}_2 &= [\tau_{comb,2}, \dots, \tau_{comb,4}, \tau_{load}] \\ \Phi &= e^{A\Delta t}\end{aligned}\quad (13)$$

The sampling time Δt depends on the mean engine speed $\bar{\omega}$ and crank angle resolution $\Delta\varphi$:

$$\Delta t = \frac{\Delta\varphi}{\bar{\omega}} \quad (14)$$

The fluctuations of the engine speed can be neglected. The unknown inputs \underline{u}_2 described before are substituted by the values obtained from the combustion and load torque models. The unknown parameters $\underline{\xi}$ are formulated as states:

$$\begin{pmatrix} \underline{x}_{k+1} \\ \underline{\xi}_{k+1} \end{pmatrix} = \begin{bmatrix} \Phi \underline{x}_k + B_1 \underline{u}_1 + B_2 \begin{bmatrix} 0 \\ \tau_{comb,2}(\delta_{1,k}) \alpha_{1,k} \\ \tau_{comb,3}(\delta_{2,k}) \alpha_{2,k} \\ \tau_{comb,4}(\delta_{3,k}) \alpha_{3,k} \\ 4 \times \tau_{ind,1} \gamma_k \end{bmatrix} \\ \underline{\xi}_k \end{bmatrix} \quad (15)$$

The structure of the new design model can be summarized using a nonlinear system function $f(\underline{x})$ and a new input matrix B . The parameter vector $\underline{\xi}_k$ contains the combustion and load torque parameters $\underline{\vartheta}_l$ and γ . Measurement and modelling uncertainty are assumed to be white Gaussian noise. This leads to the following stochastic design model for a parameter and state estimator:

$$\begin{aligned} \tilde{\underline{x}}_{k+1} &= \underline{f}(\tilde{\underline{x}}_k) + B \tilde{\underline{u}}_k + \underline{v}_k \\ \underline{y}_k &= C \tilde{\underline{x}}_k + \underline{n}_k \end{aligned} \quad (16)$$

with the new state and input vectors:

$$\begin{aligned} \tilde{\underline{u}} &= [\tau_{ind,1} + \tau_{mass,1}, \tau_{comp} + \tau_{mass,2}, \dots, \tau_{comp} + \tau_{mass,4}]^T \\ \tilde{\underline{x}} &= [\underline{x}^T, \underline{\xi}^T]^T \end{aligned} \quad (17)$$

and white Gaussian process noise \underline{v}_k and measurement noise \underline{n}_k . Process and measurement noise are furthermore mutually independent ($E\{\underline{v}_k \underline{n}_k^T\} = 0$).

3.2 Dual estimation with the Extended and Unscented Kalman Filters

For the dual estimation problem of states and parameters in (16) the EKF and the UKF are compared. For a detailed description of both algorithms the reader is referred to [9], [10], [11] and [12].

The measurement equation in (16) is linear. However, due to the nonlinearity of the system function $\underline{f}(\underline{x})$ a Jacobian matrix and the unscented transformation of $\underline{f}(\underline{x})$ are necessary for the EKF and the UKF respectively. The nonlinear system function $\underline{f}(\underline{x})$ contains the data-derived combustion torque from the cylinder 1 pressure. Hence, no analytic description of the system function is known. In order to obtain the Jacobian for the EKF the data-derived system function $\underline{f}(\underline{x})$ is linearly interpolated and then numerically differentiated. The unscented transformation doesn't need the calculation of a Jacobian. Furthermore it delivers a higher accuracy of mean and covariance estimates of the system states under assumptions of white, Gaussian noise (second order compared to first order Taylor series approximation of the EKF).

The initialization of both filters is adjusted according to the cylinder-wise combustion segments. This means that the initial error covariance matrix, as well as the starting parameters $\underline{\vartheta}_0$ are reset to the conditions of cylinder 1 ($\delta = 0, \alpha = 1, \gamma = 1$) after each combustion cycle. Table 1 illustrates the firing of the four cylinders and the resulting segmentation into four combustion segments of 180 CAD.

Combustion cylinder 2	Combustion cylinder 1	Combustion cylinder 3	Combustion cylinder 4
-180 ... 0 [CAD]	0 ... 180 [CAD]	180 ... 360 [CAD]	360 ... 540 [CAD]
Estimation of α_2, δ_2	Estimation of γ	Estimation of α_3, δ_3	Estimation of α_4, δ_4

Table 1. Combustion segmentation and the resulting order of parameter estimations

The estimation algorithm starts with the cylinder 2 parameter estimation. In segment 2 only the load torque parameter γ is estimated, since the combustion torque of cylinder 1 is known. After this segment, the load torque is updated with γ and kept constant for the following three combustion segments. In segments 3,4 the parameters of cylinders 3,4 are estimated. At the beginning of each segment, the error covariance matrix of the estimated parameters is reinitialized to starting conditions. This procedure is repeated for every operating cycle.

4. EXPERIMENTS USING A FOUR CYLINDER ENGINE TEST BED

In order to validate the performance of the Extended and the Unscented Kalman Filter approaches, a four-cylinder engine test bed was used. The pressure measurements were available in a resolution of 1 CAD. Engine speed measurements were available with 1 CAD resolution at the free end (optical sensor) and 6 CAD resolution at the flywheel (60-2 toothed gear).

EKF and UKF estimates were analyzed for different operating points. Figures 4 and 5 show the performance of EKF and UKF at 2000 rpm and 8 bar load for 50 operating cycles. Pressure measurements are used to calculate the combustion torque reference. EKF and UKF peak and phase estimates are equally good. The minor difference in EKF and UKF estimates are insignificant with respect to the resolution. One reason for the equally good results of EKF and UKF may be the linear measurement equation which reduces the nonlinearity of the problem. This result was confirmed by measurements at other operating points.

5. CONCLUSIONS

This work showed a comparison of UKF and EKF for cylinder-wise torque estimation considering engine speed fluctuations at both ends of the crankshaft. In order to account for torsional deflections, a multi-body model of the crankshaft was applied. For system inversion, a parametric torque model was obtained through one cylinder pressure measurement. Its parameters were estimated using the EKF and the UKF. They showed equally good performance for peak and phase estimates.

This study analyzed the feasibility of the EKF and UKF approach without computational considerations related to a series production. Future work will focus on improved crankshaft modelling, as well as on a different inversion strategy for torque estimation.

REFERENCES

- [1] Giorgio Rizzoni, "Estimate of indicated torque from crankshaft speed fluctuations: A model for the dynamics of the IC engine," *IEEE Transactions on Vehicular Technology*, vol. 38, No.3, pp. 168–179, 1989.
- [2] Hermann Fehrenbach, "Berechnung des Brenndruckverlaufes aus der Kurbelwellen-Winkelgeschwindigkeit von Verbrennungsmotoren," *Fortschrittsberichte VDI*, vol. 22a 2960-255, pp. 1–141, 1991.
- [3] Ruben Villarino and Johann F. Böhme, "Pressure reconstruction and misfire detection from multichannel structure-borne sound," *ICASSP'04*, vol. 2, pp. 141–144, 2004.
- [4] Stefan Larsson and Stefan Schagerberg, "SI-engine cylinder pressure estimation using torque sensors," *Society of Automotive Engineers*, vol. 2004-01-1369, pp. 401–410, 2004.
- [5] Haris Hamedovic, Franz Raichle, Jörg Breuninger, Wolfgang Fischer, Werner Dieterle, and Martin Klenk, "IMEP-estimation and in-cylinder pressure reconstruction for multicylinder SI-engine by combined processing of engine speed and one cylinder pressure," *Society of Automotive Engineers*, vol. 2005-05P-62, pp. 1–8, 2005.
- [6] Haris Hamedovic, Franz Raichle, and Johann F. Böhme, "In-cylinder pressure reconstruction for multicylinder si-engine by combined processing of engine speed and one cylinder pressure," *Proc. IEEE-ICASSP'05*, 2005.
- [7] Stefan Schagerberg and Tomas McKelvey, "Instantaneous crankshaft torque measurements - modeling and validation," *Society of Automotive Engineers*, vol. 2003-01-0713, pp. 157–172, 2003.
- [8] Stefan Schagerberg, "Torque sensors for engine applications," Tech. Rep., Department of Signals and Systems School of Electrical Engineering Chalmers University of Technology, 2003.
- [9] R. E. Kalman, "A new approach to linear filtering and prediction problems," *Trans. ASME J. Basic Eng.*, vol. 82, pp. 34–45, 1960.
- [10] Mohinder S. Grewal and Agnus P. Andrews, *Kalman Filtering Theory and Practice using MATLAB*, A Wiley-Interscience Publication, 2001.
- [11] Simon J. Julier and Jeffrey K. Uhlmann, "Unscented filtering and nonlinear estimation," *Proceedings of the IEEE*, vol. 92, pp. 401–422, 2004.
- [12] Eric A. Wan and Rudolph van der Merwe, "The unscented Kalman filter for nonlinear estimation," *Proceedings of Symposium 2000 on Adaptive Systems for Signal Processing Communication and Control*, *IEEE*, pp. 1–6, 2000.

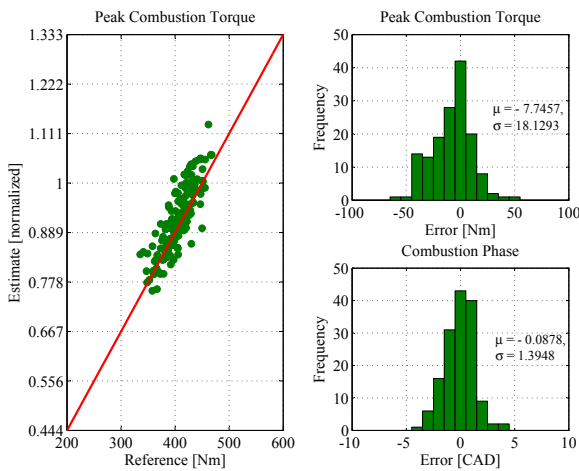


Fig. 4. Extended Kalman Filter, 2000 rpm and 8 bar load, 50 operating cycles: (a) Estimated peak of the combustion torque. (b) Combustion phase error of the estimated combustion torque

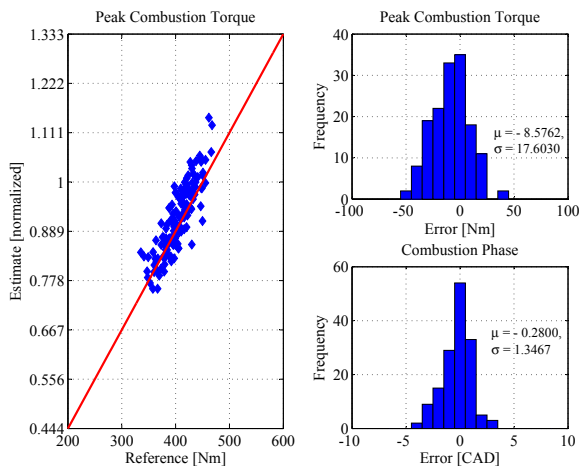


Fig. 5. Unscented Kalman Filter, 2000 rpm and 8 bar load, 50 operating cycles: (a) Estimated peak of the combustion torque. (b) Combustion phase error of the estimated combustion torque